Electronic Structure and Fermiology of $PuCoGa_5$

Takahiro Maehira[1], Takashi Hotta[1], Kazuo Ueda[2,1], and Akira Hasegawa[3]
[1] *Advanced Science Research Center, Japan Atomic Energy Research Institute, Tokai, Ibaraki 319-1195, Japan*
[2] *Institute for Solid State Physics, University of Tokyo, Kashiwa, Chiba 277-8581, Japan*
[3] *Niigata University, Niigata, Niigata 950-2181, Japan*

(Dated: February 1, 2008)

By using a relativistic linear augmented-plane-wave method, we clarify energy band structures and Fermi surfaces of recently discovered plutonium-based superconductor $PuCoGa_5$. We find several cylindrical sheets of Fermi surfaces with large volume, very similar to $CeMIn_5$ (M=Ir and Co) isostructural with $PuCoGa_5$, in spite of different f-electron numbers between Ce^{3+} and Pu^{3+} ions. The similarity is understood by a concept of electron-hole conversion in a tight binding model constructed based on the j-j coupling scheme. Based on the present results, we provide a possible scenario to explain why a transition temperature is so high as 18.5K in $PuCoGa_5$.

PACS numbers: 74.25.Jb, 74.70.Tx, 71.18.+y, 71.15.Rf

Recently it has been discovered that $PuCoGa_5$ exhibits superconductivity [1]. Surprisingly its superconducting transition temperature T_c is 18.5K, which is the highest among those yet observed f-electron materials and high enough even compared with other well-known intermetallic compounds. It has been also found that $PuRhGa_5$ becomes superconducting with T_c=8.6K [2]. These plutonium intermetallic compounds $PuMGa_5$ have the same $HoCoGa_5$-type tetragonal structure as $CeMIn_5$, a family of cerium-based heavy fermion superconductors [3]. Note, however, that superconductivity occurs for M=Ir (T_c=0.4K) and Co (2.3K) in $CeMIn_5$, while antiferromagnetic (AFM) phase has been found for M=Rh at ambient pressure. Another isostructural material including uranium is $UMGa_5$ [4], but superconductivity has not been found yet. These $HoCoGa_5$-type compounds are frequently referred to as "115".

Regarding superconducting mechanism in the 115 compounds, first let us consider Ce-115. It has been widely considered that it is unconventional d-wave superconductor induced by AFM spin fluctuations. In fact, there are some evidences such as T^3 behavior in nuclear relaxation rate [5] and node structure measured by thermal conductivity [6]. For the phase diagram of $Ce(Co,Rh,Ir)In_5$ [7], AFM phase is found to exist in adjacent to the superconducting phase. Those experimental facts remind us of high-T_c cuprates, but a clear difference from cuprates should be remarked. Namely, high-T_c superconductivity in cuprates occurs by hole doping into AFM insulators, while in Ce-115, *no* hole doping is needed. To understand the appearance of superconductivity induced by AFM spin fluctuations *without* hole doping, a crucial role of orbital degree of freedom has been pointed out by Takimoto *et al.* [8].

Concerning Pu-115, it is still premature to draw a definitive conclusion about the mechanism of superconductivity, but we notice that some normal-state properties in $PuMGa_5$ seem to be dominated by AFM spin fluctuations, e.g., the Curie-Weiss behavior in magnetic susceptibility and electric resistivity in proportion to $T^{1.35}$ [1]. Thus, it may be natural to consider that superconductivity in Pu-based compounds is also induced by AFM fluctuations. However, several problems still exist, even if d-wave superconductivity is confirmed in both Ce-115 and Pu-115 materials. One question is, of course, why T_c is so high in Pu-115. As is well known, due to difference in spatial extension of wavefunctions, $5f$ electrons have intermediate nature between localized $4f$ and itinerant $3d$ electrons. Namely, energy scale of $5f$-electrons should be larger than that of $4f$-electrons, leading to higher T_c in $5f$ electron systems if we assume the same electronic mechanism for superconductivity. However, this cannot be the whole story and the situation is not so simple, since Pu^{3+} ion includes five f-electrons, in contrast to one f-electron in Ce^{3+} ion. Furthermore one has to address the question why U-115 does *not* exhibit superconductivity. If we follow the above scenario about energy scale, U-115 can be superconducting with relatively high T_c, but that is not the case. Thus, it is *not* sufficient to consider Pu-115 and U-115 as simple analogues to Ce-115 with large energy scale, based only on difference in itinerant nature between $4f$- and $5f$-electrons.

In this Letter, in order to clarify those points, we calculate energy band structures and Fermi surfaces for $PuCoGa_5$ by applying a relativistic linear augmented-plane-wave (RLAPW) method. It is found that several sheets with large volume form cylindrical Fermi surfaces, quite similar to $CeMIn_5$ (M=Ir and Co) [10]. The whole energy scale in the band structure of $PuCoGa_5$ is larger than that of $CeMIn_5$, as naively expected. On the other hand, for $UCoGa_5$, we have found only several small pocket Fermi surfaces to show semi-metal like behavior [11], consistent with the fact that $UMGa_5$ is *not* superconducting. The similarity between Ce-115 and Pu-115 is understood by a simple tight-binding model constructed based on the j-j coupling scheme [12]. A remarkable fact is that Pu-115 can be regarded as a hole version of Ce-115. Thus, we can conclude that both Ce-115 and Pu-115 have the same electronic origin for superconductivity, suggesting that Pu-115 has higher T_c due to the combination of the electron-hole conversion concept and the energy-scale discussion.

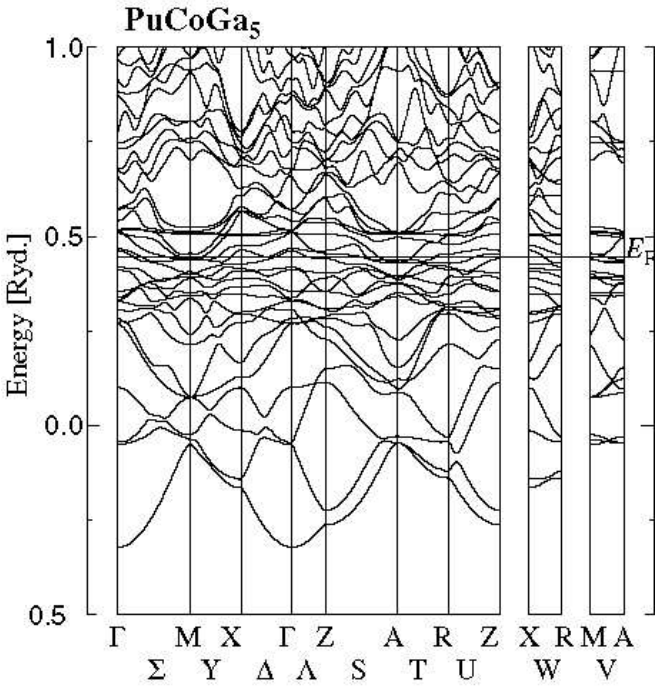

FIG. 1: Energy band structure for $PuCoGa_5$ obtained by the RLAPW method. E_F denotes the position of the Fermi level.

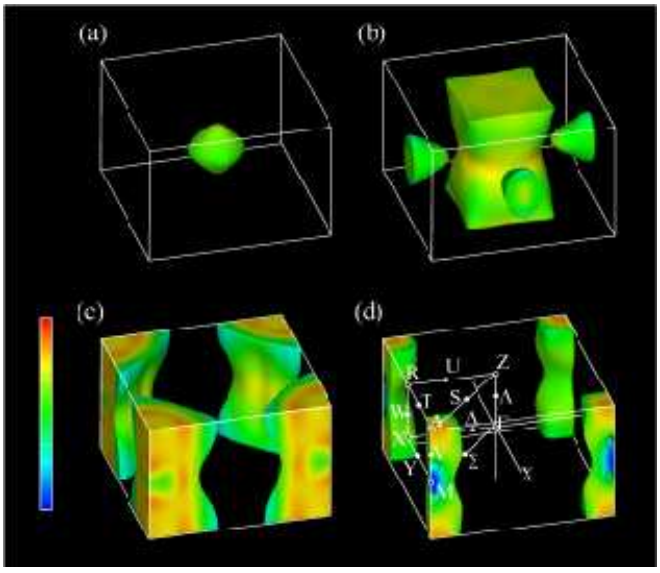

FIG. 2: Calculated Fermi surfaces of $PuCoGa_5$ for (a) 15th band hole sheets, (b) 16th band hole sheets, (c) 17th band electron sheets, and (d) 18th band electron sheets. Colors indicate the amount of $5f$ angular momentum character on each Fermi surface sheet and red-shift indicate the increase of the f charcter. The center of the Brillouin zone is set at the Γ point.

First let us briefly explain the RLAPW method. Readers interested in the formalism can consult with Refs. [13]. When we calculate the electronic energy band structure of $4f$ and $5f$ compounds, in general, relativistic effects should be included, since electrons near the heavy nucleus must move with a high speed to keep their stationary motion. In order to take into account major relativistic effects such as the relativistic energy shifts, the relativistic screening effects, and the spin-orbit interaction, Loucks derived a relativistic augmented-plane-wave method based on the Dirac one-electron wave equation [14]. Several problems in his method have been improved by Hasegawa and co-workers [13]. The local density approximation is used for the exchange and correlation potential and spatial shape of one-electron potential is determined in the muffin-tin approximation. Self-consistent calculations are performed by using the lattice constants determined experimentally [1].

In Fig. 1, we show the energy band structure for $PuCoGa_5$ along the symmetry axes in the Brillouin zone in the range from −0.5Ryd. to 1.0Ryd., where Ryd. indicates Rydberg and 1Ryd.=13.6eV. First note that in the vicinity of the Fermi level E_F located at 0.446 Ryd., there occurs hybridization between Pu $5f$ and Ga $4p$ states. Above E_F near the M point, the flat $5f$ bands split into two groups, corresponding to the total angular momentum j=5/2 (lower bands) and 7/2 (upper bands). The magnitude of the splitting Δ between the two groups is estimated as Δ(Pu)=1 eV, which is almost equal to the spin-orbit splitting in the atomic $5f$ state of Pu. Note that each Pu APW sphere contains about 5.2 electrons in the f state, suggesting that valence of plutonium ion is Pu^{3+}, consistent with experimental result [1].

By using the total density of states at E_F, evaluated as $N(E_F)$=97.3 states/Ryd.cell, the theoretical specific heat coefficient γ_{band} is estimated as 16.9 mJ/K^2·mol, while the experimental electronic specific heat coefficient γ_{exp} is 77 mJ/K^2·mol [1]. If we define the enhancement factor for the electronic specific heat coefficient as $\lambda=\gamma_{exp}/\gamma_{band}-1$, we obtain λ=3.6, which is smaller than λ=10 for $CeCoIn_5$ [10]. Note that the enhancement of λ from unity is a measure of electron correlation effect. The moderate λ in Pu-115 suggests that the correlation effect in Pu-115 should be weak compared with Ce-115. Since localized nature is stronger in $4f$ electrons, the correlation effect is more significant in Ce-115.

Now we discuss the Fermi surfaces of $PuCoGa_5$. In Fig. 1, the lowest fourteen bands are fully occupied. The next four bands are partially occupied, while higher bands are empty. Then, as shown in Figs. 2(a)-(d), 15th, 16th, 17th, and 18th bands crossing the Fermi level construct the hole or electron sheets of the Fermi surfaces, summarized as follows: (a) The Fermi surface from the 15th band includes one small hole sheet centered at the Γ point. (b) The 16th band constructs a large cylindrical hole sheet centered at the Γ point, while two equivalent small hole sheets are centered at X points. Depending on the energy resolution in the calculation, it is subtle whether those two hole sheets touch each other or not, but in any case, the quasi two-dimensional large hole sheet centered at the Γ point gives the main contribu-

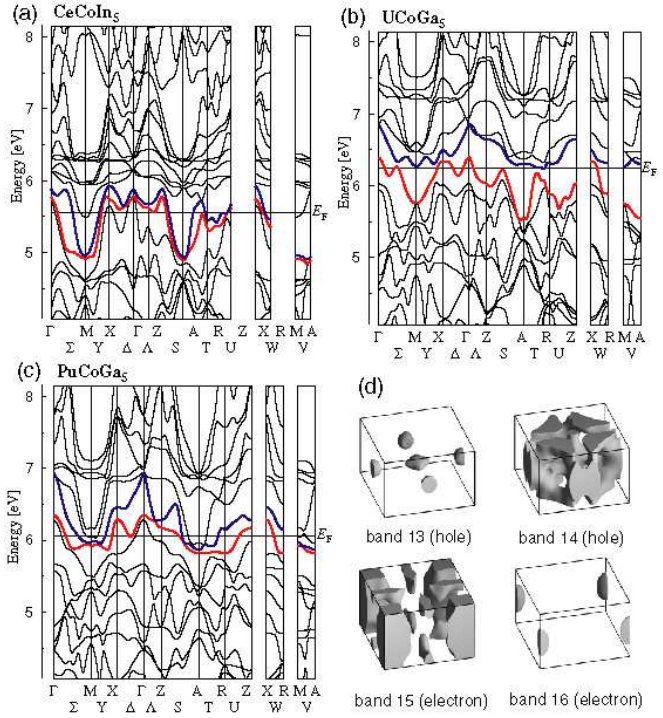

FIG. 3: Energy band structure around $E_{\rm F}$ for (a) $CeCoIn_5$, (b) $UCoGa_5$, and (c) $PuCoGa_5$. In each panel, red and blue curves indicate the upper and lower bands to construct the hole and electron Fermi-surface sheets, respectively. Namely, those are 14th (red) and 15th (blue) for $CeCoIn_5$, 15th (red) and 16th (blue) for $UCoGa_5$, and 16th (red) and 17th (blue) for $PuCoGa_5$. (d) Calculated Fermi surfaces of $CeCoIn_5$.

tion. (c) The 17th band has a large cylindrical electron sheet centered at the M point. (d) The 18th band provides another cylindrical electron sheet centered at the M point.

Let us consider the main Fermi surfaces from the viewpoints of the Fermi-surface volume and f-electron admixture. As for the Fermi surface constructed from 18th band, f-electrons are not uniformly distributed on it, as expressed in color scale. Around the A-point, f-electron admixture is large, while p-electron gives a large contribuation around the M-point. If we ignore three dimensionality and small-volume Fermi surfaces, the main contributors are the hole sheet from the 16th band centered at the Γ point and the electron sheet from the 17th band centered at the M point.

In order to gain deeper insight into electronic structure of Pu-115, it is instructive to compare with the results for Ce-115 [10] and U-115 [11]. In Figs. 3 (a)-(c), we show the energy band structures around $E_{\rm F}$ for $CeCoIn_5$, $UCoGa_5$, and $PuCoGa_5$, respectively, in the same energy scale. Note that $CeCoIn_5$ becomes superconducting with $T_{\rm c}$=2.3K [3], while $UCoGa_5$ is Pauli paramagnet [4]. First, we can estimate Δ(Ce)=0.4eV and Δ(U)=0.8eV, which are almost equal to the spin-orbit splittings in the atomic $4f$ and $5f$ states for Ce and U, respectively. As expected, we obtain $\Delta({\rm Ce})<\Delta({\rm U})\lesssim\Delta({\rm Pu})$. As shown in the figure caption, the number to label red and blue curves increase one by one in the order of $CeCoIn_5$, $UCoGa_5$, and $PuCoGa_5$, corresponding to the increase in f-electron number by two per site. Note that shapes of red and blue curves among three 115 compounds are similar to one another, since overall band structure around the Fermi level is always determined by hybridization between broad p-bands and narrow f-bands for 115 compounds. The center of gravity of the j=5/2 states in $CeCoIn_5$ is about 0.4eV above $E_{\rm F}$, while the center of those in $PuCoGa_5$ is slightly lower than $E_{\rm F}$. Concerning $UCoGa_5$, the j=5/2 states seem to be just at the Fermi energy. This trend is consistent with the number of f-electrons in each compounds. The width of j=7/2 and 5/2 bands around at the M- or A-points becomes broad in the order of $CeCoIn_5$, $UCoGa_5$, and $PuCoGa_5$, consistent with the difference in $4f$- and $5f$-electron wavefunctions.

Here we emphasize that Ce-115 and Pu-115 exhibit large Fermi suafces, as shown in Figs. 2 and 4(d). In particular, we see a clear similarity between main Fermi surfaces of $CeCoIn_5$ and $PuCoGa_5$, except for fine structures. Considering only f-electron dominant Fermi surface with large volume, we observe in common the large hole sheet centered at the Γ point and the large cylindrical electron sheet centered at the M point. On the other hand, U-115 has small-pocket Fermi surfaces, as deduced from Fig. 2(b) [11]. Namely, U-115 is considered as a semi-metal, which seems to be closely related to the reason why U-115 does not exhibit superconductivity. The origin of the semi-metallic behavior may be traced back to slight overlap among the j=5/2 f-bands strongly hybridized with the p-states from Ga ions.

In order to understand the similarity in energy band structures and Fermi surfaces between Ce-115 and Pu-115, it is convenient to reanalyze the tight-binding model obtained based on the j-j coupling scheme [12]. To consider the 115 systems, we include only f- and p-electrons in the two-dimensional network composed of Ce and In (Pu and Ga) ions [10]. Due to the lack of space, we skip the details of the model for j=5/2 sextet [10, 12], but the Hamiltonian H is written as $H=H_{\rm f}+H_{\rm p}+H_{\rm fp}$, where $H_{\rm f}$, $H_{\rm p}$, and $H_{\rm fp}$ are, respectively, f-electron hopping, p-electron hopping, and f-p hybridization terms, which are characterized by the Slater integrals $(ff\sigma)$, $(pp\sigma)$, and $(fp\sigma)$, respectively. Note that crystalline electric field terms are simply ignored, since those are much smaller than the energies considered here.

In Fig. 4(a), we show the direct comparison between the RLAPW and tight-binding results for $(ff\sigma)$=4500K, $(fp\sigma)$=6000K, and $(pp\sigma)$=18630K. Top and bottom of the tight-binding bands are determined by comparison with the RLAPW ones with significant amount of Ga $4p$ states. The Fermi level for H is determined so as to include five f electrons. First, overall features of the bands in the vicinity of $E_{\rm F}$ are well reproduced by the mixture of broad p- and narrow f-bands. Second, magnitude of parameters for $PuCoGa_5$ are large compared

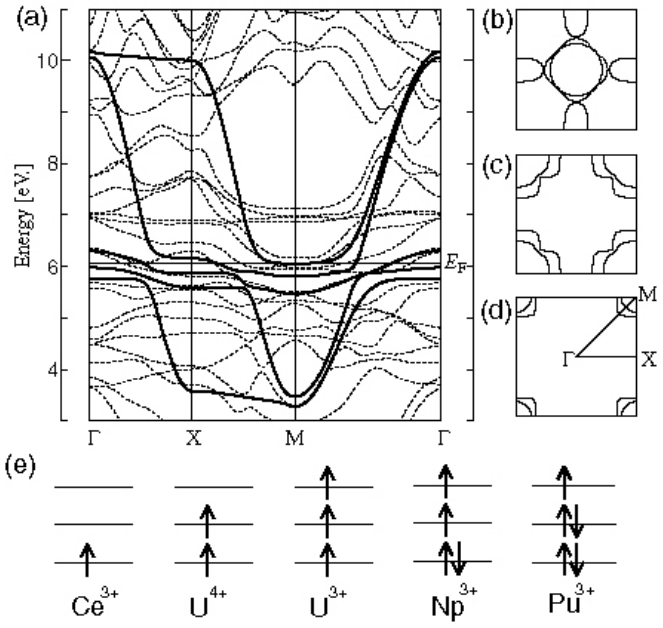

FIG. 4: (a)Energy band structures for $PuCoGa_5$ around E_F for the tight-binding model (solid curves) and the RLAPW results(dashed curves). Fermi-surface lines discussed here are (b)16th band hole sheets, (c)17th band electron sheets, and (d)18th band electron sheets. Note that solid and broken curves denote the tight-binding and RLAPW Fermi surfaces, respectively. (e) Configurations for f-electrons accommodated in three Kramers doublets. Up and down arrows denote pseudo-spin up and down, respectively.

with those for $CeCoIn_5$, $(ff\sigma)$=4400K, $(fp\sigma)$=5360K, and $(pp\sigma)$=5730K [10]. Note that the difference in $(pp\sigma)$ between $PuCoGa_5$ and $CeCoIn_5$ is mainly due to the difference of Ga $4p$ and In $5p$ electronic states. Then, we conclude that $5f$ electrons are more itinerant than $4f$ ones from the present results for tight-binding fitting. As shown in Figs. 4(b)-(d), the main Fermi surfaces are well reproduced by the tight-binding model. Good agreements between RLAPW and tight-binding results indicate the validity of the j-j coupling scheme for $PuCoGa_5$.

In the tight-binding model constructed based on the j-j coupling scheme, we are allowed to consider the f^n configuration with n>2 by accommodating n electrons among three Kramers doublets. In Fig. 4(e), we show several f-electron configurations. First of all, we note the electron-hole conversion relation between Ce^{3+} and Pu^{3+} ions [12]. Thus, Pu-115 can be considered as a hole version of Ce-115 and this is the very reason why common Fermi surfaces are observed.

Note that $UMGa_5$ has been found to be AFM metal for M=Ni, Pd, and Pt, while Pauli paramagnetic for M=Fe, Co, and Rh [4]. Thus, the present band-structure calculation assuming the paramagnetic phase is consistent with the experimental result for $UCoGa_5$. On the other hand, a hint to understand AFM metallic behavior for M=Ni, Pd, and Pt may be found in the local spin structure. Although it is difficult to determine the exact valence of uranium ion, it should be between U^{4+} and U^{3+}. As shown in Fig. 4(e), for U^{4+} (U^{3+}) ion, local spin S=1 (3/2) may be formed due to the Hund's rule coupling and thus, the AFM phase will be favored. However, it is still an open problem to explain the metallic behavior in the AFM phase as well as the difference in the AFM spin structure between $UPtGa_5$ and $UNiGa_5$ [4].

Finally, we provide one short comment on Np-115. For Np^{3+} ion, as shown in Fig. 4(e), we can regard it as a hole version of U^{4+} and thus, Np-115 may not exhibit superconductivity, but antiferromagnetism or paramagnetism, as an analogue of U-115.

In summary, we have performed the band-structure calculation for $PuCoGa_5$ and obtained the Fermi surfaces similar to Ce-115 materials. This similarity can be understood by the electron-hole conversion picture based on the j-j coupling scheme. We believe that high T_c in $PuCoGa_5$ can be understood by combining our electron-hole picture with the energy-scale difference in $4f$- and $5f$-electrons.

We thank Y. Ōnuki, J. L. Sarrao, T. Takimoto, F. Wastin, and H. Yamagami for discussions. T. H. and K. U. are supported by the Grant-in-Aid for Scientific Research from Japan Society for the Promotion of Science.

[1] J. L. Sarrao *et al.*, Nature (London) **420**, 297 (2002).
[2] F. Wastin *et al.*, preprint.
[3] H. Hegger *et al.*, Phys. Rev. Lett. **84**, 4986 (2000); C. Petrovic *et al.*, Europhys. Lett. **53**, 354 (2001); C. Petrovic *et al.*, J. Phys.: Condens. Matter. **13**, L337 (2001).
[4] Y. N. Grin *et al.*, J. Less. Common Met. **121**, 497 (1986); Y. Ōnuki *et al.*, Acta Phys. Pol. B**32**, 3273 (2001); Y. Tokiwa *et al.*, J. Phys. Soc. Jpn. **70**, 2982 (2001); Y. Tokiwa *et al.*, J. Phys. Soc. Jpn. **71**, 845 (2002); H. Kato *et al.*, J. Phys. Chem. Solids **63**, 1197 (2002).
[5] Y. Kohori *et al.*, Eur. Phys. J. B**18**, 601 (2000); G.-q. Zheng *et al.*, Phys. Rev. Lett. **86**, 4664 (2001).
[6] K. Izawa *et al.*, Phys. Rev. Lett. **87**, 057002 (2001).
[7] P. G. Pagliuso *et al.*, Physica B**312-313**, 129 (2002).
[8] T. Takimoto *et al.*, J. Phys.: Condens. Matter. **14**, L369 (2002).
[9] T. Moriya and K. Ueda, Adv. Phys. **49**, 555 (2000).
[10] T. Maehira *et al.*, J. Phys. Soc. Jpn. Suppl. **71**, 285 (2002); T. Maehira *et al.*, cond-mat/0211360.
[11] T. Maehira *et al.*, cond-mat/0207575.
[12] T. Hotta and K. Ueda, cond-mat/0211467.
[13] A. Hasegawa and H. Yamagami, Prog. Theor. Phys. Suppl. **108**, 27 (1992); H. Yamagami and A. Hasegawa, J. Phys. Soc. Jpn. **59**, 2426 (1990); M. Higuchi and A. Hasegawa, J. Phys. Soc. Jpn. **64**, 830 (1995).
[14] T. L. Loucks, *Augmented Plane Wave Method* (Benjamin, New York, 1967).